Asian Journal of Andrology (2022) 24, 102–108
www.asiaandro.com; www.ajandrology.com

Open Access

ORIGINAL ARTICLE

Male Health

Polymerase chain reaction-based assays facilitate the breeding and study of mouse models of Klinefelter syndrome

Hai-Xia Zhang[1,*], Yu-Lin Zhou[1,*], Wen-Yan Xu[1], Xiao-Lu Chen[1], Jia-Yang Jiang[2], Xiao-Man Zhou[1], Zeng-Ge Wang[3], Rong-Qin Ke[2], Qi-Wei Guo[1]

Klinefelter syndrome (KS) is one of the most frequent genetic abnormalities and the leading genetic cause of nonobstructive azoospermia. The breeding and study of KS mouse models are essential to advancing our knowledge of the underlying pathological mechanism. Karyotyping and fluorescence *in situ* hybridization are reliable methods for identifying chromosomal contents. However, technical issues associated with these methods can decrease the efficiency of breeding KS mouse models and limit studies that require rapid identification of target mice. To overcome these limitations, we developed three polymerase chain reaction-based assays to measure specific genetic information, including presence or absence of the sex determining region of chromosome Y (*Sry*), copy number of amelogenin, X-linked (*Amelx*), and inactive X specific transcripts (*Xist*) levels. Through a combined analysis of the assay results, we can infer the karyotype of target mice. We confirmed the utility of our assays with the successful generation of KS mouse models. Our assays are rapid, inexpensive, high capacity, easy to perform, and only require small sample amounts. Therefore, they facilitate the breeding and study of KS mouse models and help advance our knowledge of the pathological mechanism underlying KS.

Asian Journal of Andrology (2022) **24**, 102–108; doi: 10.4103/aja.aja_38_21; published online: 28 May 2021

Keywords: 40,XX^{Y*} mouse; 41,XXY mouse; Klinefelter syndrome; mouse model

INTRODUCTION

Klinefelter syndrome (KS), a set of symptoms that results from an extra X chromosome in males, is one of the most frequent genetic abnormalities and the leading cause of nonobstructive azoospermia.[1] The prevalence of KS in newborn, infertile, and azoospermic males is approximately 0.15%, 3%–4%, and 10%–12%, respectively.[2,3] The phenotypic spectrum of KS is wide, ranging from manifesting only as small testes and infertility to more classic traits and comorbidities, such as hypergonadotropic hypogonadism, infertility, neurocognitive deficits, psychiatric disorders, obesity, diabetes, osteoporosis, and autoimmune disorders.[4–8] Early diagnosis of KS and subsequent treatment and intervention, such as testosterone replacement therapy, testicular sperm extraction, early speech and occupational therapy, and educational assistance, have been shown to improve the long-term quality of life for patients with KS and alleviate later complications.[9–15] However, the existing data are limited, and more rigorous scientific investigations are needed.[16] In fact, the pathological mechanism underlying the aforementioned phenotypes and the extra X chromosome is much more complicated than previously envisioned and remains mostly unknown,[8,17,18] in large part because in-depth investigations, such as developmental studies and experimental manipulations, are nearly impossible to perform in patients with KS for ethical reasons.[16,19] Therefore, animal model studies are essential to advancing our knowledge of the pathological mechanism underlying this prevalent syndrome.[19]

The discovery of a mutant mouse line, the Y* mouse, has enabled us to generate KS mouse models.[20] As shown in **Figure 1**, the Y* chromosome contains the X-centromere, partial pseudoautosomal region (PAR) of the X chromosome, partial PAR of the Y chromosome, and the entire nonrecombining region of the Y chromosome (NRY). In addition, a small fragment of the nonpseudoautosomal region of the X chromosome (NPX), which contains eight genes including amelogenin, X-linked (*Amelx*), is located between the X-centromere and the duplicated PAR. Through cross-breeding, 40,XX^{Y*} and 41,XXY mice can be generated in the second and fourth generations, respectively.[21,22] These two mouse breeds possess many of the characteristics of KS, including small firm testes, germ cell loss, hypergonadotropic hypogonadal endocrine changes, altered body proportions, and behavioral and cognitive issues.[19,21,22] Therefore, these mouse breeds have been widely used as animal models to overcome the limitations of human studies and explore the pathological mechanism underlying KS.[19,21–24]

[1]United Diagnostic and Research Center for Clinical Genetics, Women and Children's Hospital, School of Medicine and School of Public Health, Xiamen University, Xiamen 361102, China; [2]School of Biomedical Sciences and School of Medicine, Huaqiao University, Quanzhou 362021, China; [3]Beijing Children's Hospital, Capital Medical University, Beijing 100045, China.
*These authors contributed equally to this work.
Correspondence: Dr. QW Guo (guoqiwei@xmu.edu.cn)
Received: 27 November 2020; Accepted: 22 March 2021

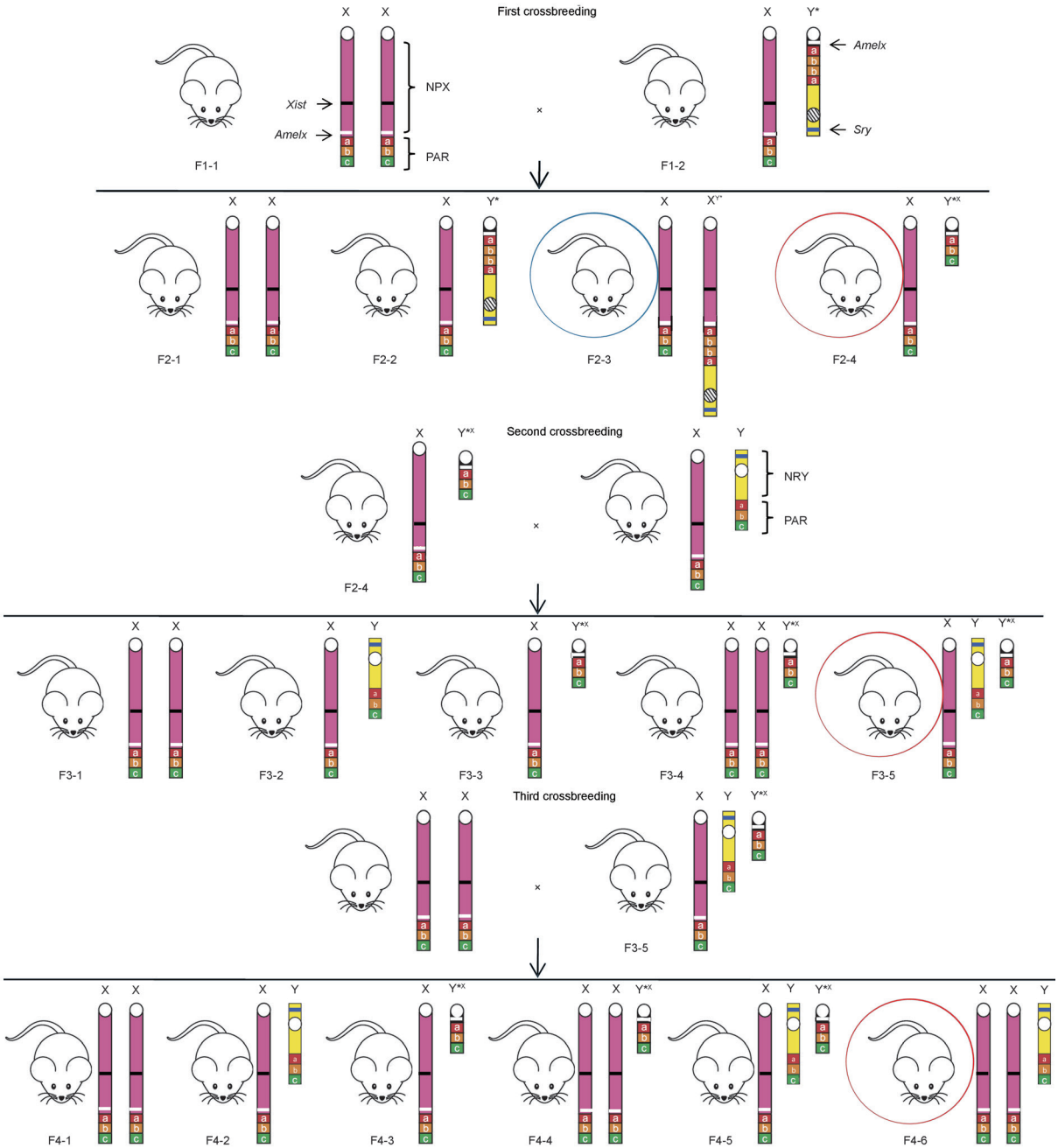

Figure 1: Breeding of KS mouse models. The mouse in the blue circle is a 40,XX^{Y*} mouse, one of the KS mouse models. The mice in the red circles are the target mice in each generation for breeding 41,XXY mice, another KS mouse model. This figure was modified from figures in a previous study.[21] NPX: nonpseudoautosomal region of the X chromosome; NRY: nonrecombining region of the Y chromosome; PAR: pseudoautosomal region. *Sry*: sex determining region of chromosome Y; *Amelx*: amelogenin, X-linked; *Xist*: inactive X specific transcripts; KS: Klinefelter syndrome.

One of the most important steps in the successful breeding of 40,XX^{Y*} and 41,XXY mice is the accurate identification of the karyotypes and chromosomal fragments of the targeted mouse breeds (**Figure 1**). This is typically performed through cytogenetic methods, such as karyotyping or fluorescence *in situ* hybridization (FISH).[22,23,25,26] To ensure that the mice are alive for subsequent breeding after testing, culture cells derived from blood samples or tissue biopsies are used.[25] However, the identification of target mice by karyotyping or FISH is labor-intensive, time-consuming (4–10 days), and requires a relatively high level of expertise.[22,23,25,26] These drawbacks reduce the usefulness of cytogenetic methods in large-scale detection, which is generally required to generate enough model mice for the study. Moreover, pathological changes in KS model mice, such as germ cell loss, occur prenatally and progress rapidly after birth.[23,27] Therefore, studies of these early pathological changes require immediate identification of target mice prenatally or neonatally; this poses a challenge for karyotyping and FISH, both of which require a relatively long turnaround time.

To overcome these limitations, we developed three polymerase chain reaction (PCR)-based assays to identify the chromosomal

contents of target mice and confirmed the utility of our assays for reliable KS mouse model breeding.

ANIMALS AND METHODS

Study design

As shown in **Figure 1**, each karyotype has specific sex chromosome contents that could provide specific genetic information, such as gene copy number and transcriptional activity. Theoretically, by analyzing this genetic information using molecular methods instead of cytogenetic analyses, such as karyotyping and FISH, we would be able to infer the karyotype of a mouse breed. On the basis of this concept, three genes, sex determining region of chromosome Y (*Sry*), *Amelx*, and inactive X specific transcripts (*Xist*), could be informative. *Sry* is located on the NRY, and its presence or absence determines the sex of the mouse. Since *Amelx* is located in the NPX and is also present on the Y^* chromosome; the copy number of *Amelx* implies the copy number of the NPX fragment.[28] *Xist* is also located on the NPX and is transcribed into a long noncoding RNA that can transcriptionally silence one of the two X chromosomes to achieve dosage equivalence between males and females. Thus, a high level of *Xist* RNA is expected when there are two X chromosomes in a single cell, whereas an absence or low level of *Xist* RNA is expected when there is only one X chromosome in a single cell.[29] Corresponding to the breeding protocol shown in **Figure 1**, the genetic information of the mouse breeds in each generation is shown in **Figure 2**. This genetic information was determined using our PCR-based assays designed to measure the presence or absence of *Sry*, the copy number of *Amelx*, and the transcript levels of *Xist* RNA. Notably, the combined information for two genes was sufficient to identify a target karyotype (**Figure 2**).

Mice and samples

To establish the PCR assays, tail tissue samples from 16 pairs of 40,XX and 40,XY mice (C57BL/6J) were obtained from the Experimental Teaching Department, School of Medicine, Xiamen University (Xiamen, China). To generate $40,XX^{Y^*}$ and 41,XXY mice, breeding pairs of $40,XY^*$ (C57BL/6JEiJ) and 40,XX (C57BL/6J) mice were purchased from The Jackson Laboratory (Bar Harbor, ME, USA). The 40,XY mice (C57BL/6J) were purchased from Xiamen University Laboratory Animal Center (Xiamen, China). Breeding was performed in the standard animal facility of the Xiamen University Laboratory Animal Center.

Nucleic acid purification

Approximately 20 mg of tail tissue was used to purify DNA or RNA with the QIAamp Fast DNA Tissue Kit (Qiagen, Valencia, CA, USA) or the RNeasy® Mini Kit (Qiagen), respectively, according to the manufacturer's protocols. The purity and concentration of the purified nucleic acid were determined by measuring the absorbance at 260 nm and 280 nm using a NanoDrop 2000 spectrophotometer (Thermo Fisher Scientific, Waltham, MA, USA).

PCR and melting conditions

PCR conditions for all assays were identical and as follows: each 25 μl reaction mixture contained 10 mmol l^{-1} Tris-HCl (pH 8.3), 50 mmol l^{-1} KCl, 1 U of TaqHS (Takara, Dalian, China), 2 mmol l^{-1} Mg^{2+}, 0.2 mmol l^{-1} of each dNTP, 0.8× LightCycler 480 ResoLight Dye (Roche Applied Science GmbH, Mannheim, Germany), 0.2 mmol l^{-1} of each forward and reverse primer, and a specific amount of DNA or complementary DNA (cDNA) template. The amplification cycling conditions were as follows: 95°C for 3 min, followed by 40 cycles at 95°C for 20 s, 60°C for 20 s, and 72°C for 20 s. Fluorescence was recorded at the end of each annealing step. The sequences of the primers used in each assay are listed in **Table 1**. For the measurement of *Sry*, melting analysis was performed after the amplification, which began with denaturation at 95°C for 1 min and renaturation at 35°C for 3 min, followed by melting from 40°C to 95°C with a ramp rate of 0.04°C s^{-1}. Fluorescence was recorded every 0.3°C. PCR and melting analysis were performed on a SLAN-96S thermocycler (Zeesan, Xiamen, China). Before PCR, RNA samples were reverse transcribed with the GoScript Reverse Transcription System (Promega, Beijing, China) according to the manufacturer's protocol, and 1 μl of the resulting cDNA was used as template for subsequent PCR.

Data analyses

For the analysis of *Sry*, a melting profile was used to determine its presence or absence. To determine the copy number of *Amelx*, relative quantification was performed by measuring the difference between the quantification cycle (Cq) values obtained for *Amelx* and actin, beta (*Actb*), as $\Delta Cq_{Amelx\ -\ Actb}$. Similarly, to evaluate *Xist* RNA transcript levels, relative quantification was performed by measuring the difference between the Cq values for *Xist* and *Actb* transcripts ($\Delta Cq_{Xist\ -\ Actb}$). *Actb* was used as a quantitative reference because it consistently has two copies and a stable transcriptional pattern in mouse cells. The Cq value is defined as the amplification cycle when the fluorescence intensity of an amplicon reaches a specific threshold.[30] On the basis of a previous study, the threshold was set to 30% of the plateau fluorescence intensity as the optimal Cq value for differentiation of different karyotypes.[31]

Karyotyping and histological analysis

To confirm the accuracy of our assays, after breeding, the karyotypes of the target mice were examined by karyotyping using hematopoietic lineage cells derived from the bone marrow according to a previous protocol.[25] For histological analysis of the testes of KS model mice, periodic acid-Schiff staining was performed on cross-sections of the seminiferous tubules according to a previous protocol.[32]

Ethics statement

Mouse breeding and experimentation were performed in accordance with international, national, and institutional guidelines for the ethical use of animals.[33] The study was approved by the Ethics Committee of Xiamen University Laboratory Animal Center (No. KY-2018-0311).

RESULTS

Establishing an assay for the detection of Sry

To determine the optimal amount of DNA template for the *Sry* detection assay, serial dilutions of DNA isolated from 40,XY (*Sry* positive) and 40,XX (*Sry* negative) mice were evaluated. A template-free control was also examined to determine the melting profiles of primer dimers. As

Table 1: Primer information for the polymerase chain reaction-based assays

Target gene	*Primer sequence*	*Amplification region (assembly: GRCm39/mm39)*
Sry	F: GCAGCTTACCTACTTACTAACA	chrY: 2662499-2662564
	R: CTGAGGTGCTCCTGGTA	
Amelx	F: CCTTCAGCCTCATCACCA	chrX: 167965017-167965122
	R: TTGGGTTGGAGTCATGGA	
Xist	F: CATCCTACCATCATCTGCTTT	chrX: 102504207-102504284
	R: GGGAAGATGACTCCAGTCT	
Actb	F: CCATGAAACTACATTCAATTCCAT	chr5:142889915-142889984
	R: TGTGTTGGCATAGAGGTCTT	

Sry: sex determining region of chromosome Y; *Amelx*: amelogenin, X-linked; *Xist*: inactive X specific transcripts; *Actb*: actin, beta; chr: chromosome; F: forward; R: reverse

shown in **Figure 3a**, the melting profiles changed with the amount of DNA template. To obtain only the *Sry* amplicon, at least 2 ng of DNA template was required for samples from the 40,XY mouse. However, for the 40,XX mouse samples, the use of a larger amount of DNA template (≥20 ng) generated nonspecific amplicons that presented similar melting profiles to those of the *Sry* amplicons. Therefore, 2 ng

Breed	F2-1	F2-2	F2-3	F2-4
Karyotype	40,XX	40,XY*	40,XX$^{Y^*}$	40,XY^{*X}
Sry	-	+	+	-
Amelx	2	2	2	2
Xist RNA	+	-	+	-

Breed	F3-1	F3-2	F3-3	F3-4	F3-5
Karyotype	40,XX	40,XY	40,XY^{*X}	41,XXY^{*X}	41,XYY^{*X}
Sry	-	+	-	-	+
Amelx	2	1	2	3	2
Xist RNA	+	-	-	+	-

Breed	F4-1	F4-2	F4-3	F4-4	F4-5	F4-6
Karyotype	40,XX	40,XY	40,XY^{*X}	41,XXY^{*X}	41,XYY^{*X}	41,XXY
Sry	-	+	-	-	+	+
Amelx	2	1	2	3	2	2
Xist RNA	+	-	-	+	-	+

Figure 2: Genetic information of the mouse breeds obtained during the breeding of Klinefelter syndrome mouse models. +: presence of *Sry* or high *Xist* RNA transcripts; –: absence of *Sry* or low/no *Xist* RNA transcripts. Pink labels indicate the target mice in each generation for the breeding of 41,XXY mice. Green labels indicate the assays required to identify the target mice in each generation. For example, in the second generation, each mouse was first tested for *Sry*, and those negative for *Sry* were further tested for *Xist* RNA transcript levels. Mice with low/no *Xist* RNA transcripts (negative results in both assays) were identified as 40,XY^{*X} mice. *Sry*: sex determining region of chromosome Y; *Amelx*: amelogenin, X-linked; *Xist*: inactive X specific transcripts.

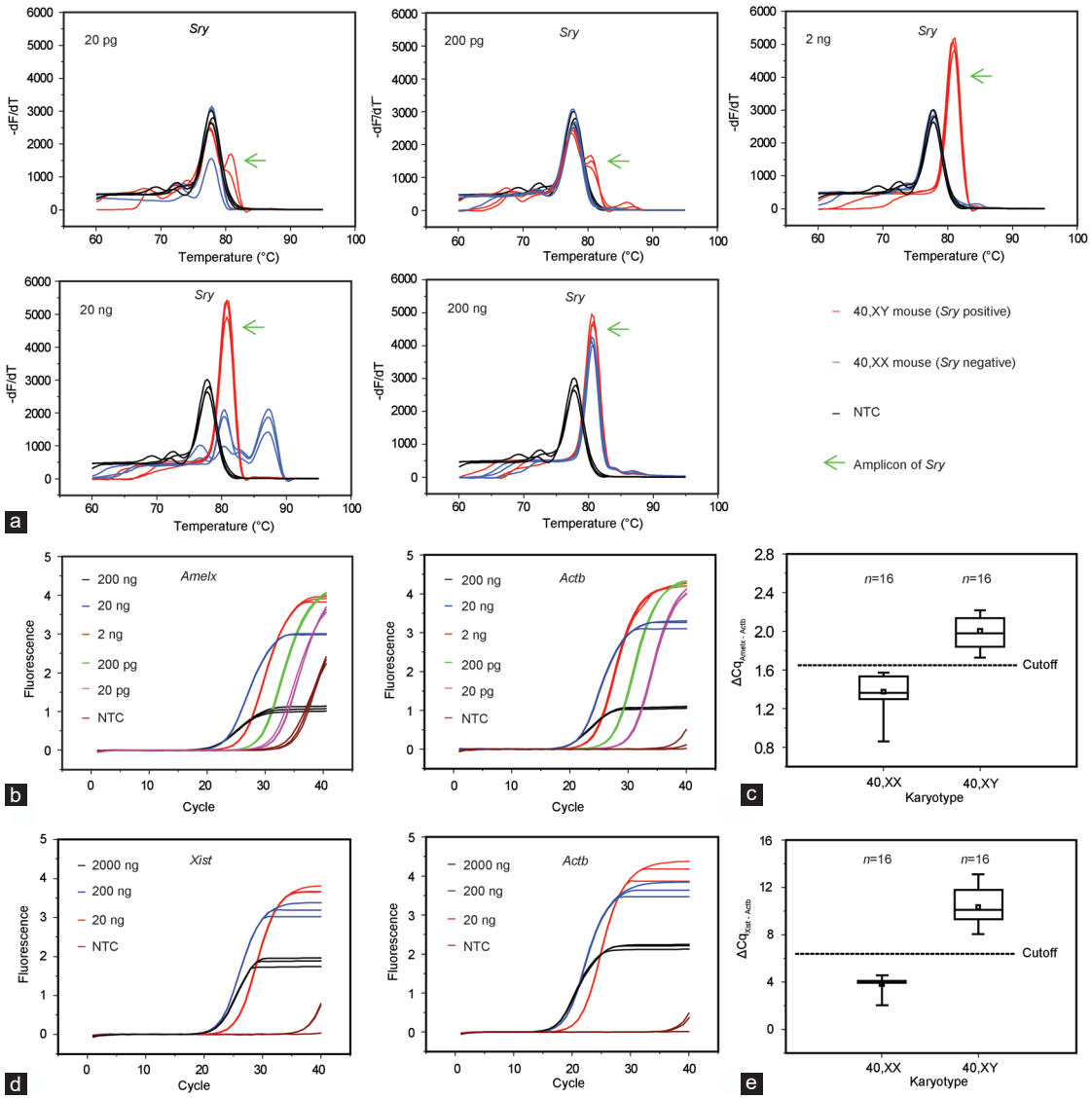

Figure 3: Polymerase chain reaction-based assays for the breeding of Klinefelter syndrome mouse models. (**a**) Melting profiles for detecting *Sry* using different amounts of DNA template. (**b**) Assays to quantify *Amelx* using different amounts of DNA template. (**c**) Establishment of a cutoff value for *Amelx* quantification. (**d**) Assays for evaluating *Xist* RNA transcript levels using different amounts of RNA template. (**e**) Establishment of a cutoff value for *Xist* RNA quantification. Each sample was tested in triplicate, and the Cq value of each sample is the mean Cq value of three replicates. NTC: no template control. *Sry*: sex determining region of chromosome Y; *Amelx*: amelogenin, X-linked; *Xist*: inactive X specific transcripts; *Actb*: actin, beta; Cq: quantification cycle.

was considered the optimal amount of template to detect specifically the presence or absence of *Sry* and was used for subsequent experiments.

Establishing an assay for the quantification of Amelx

We first evaluated the effect of the amount of DNA template on the effectiveness of the *Amelx* quantification assay by examining serial dilutions of DNA isolated from a 40,XX mouse as a template. As shown in **Figure 3b**, amplification in both the *Amelx* and *Actb* detection reactions was robust across a wide range of template concentrations (20 pg–200 ng). However, a repressive effect was observed when a relatively large amount of DNA template (≥20 ng) was used. Therefore, 2 ng was chosen as the amount of template to evaluate the ranges of $\Delta Cq_{Amelx - Actb}$ values for the 40,XX (two copies of *Amelx*) and 40,XY (one copy of *Amelx*) mouse samples. As shown in **Figure 3c**, the ranges for 16 samples of 40,XX and 40,XY mice were distinct from each other. The mean $\Delta Cq_{Amelx - Actb}$ value (1.65) of the maximum of the 40,XX samples and the minimum of the 40,XY samples was used as the cutoff value for classifying mice as having one or two copies of *Amelx* in subsequent experiments.

Establishing an assay for the evaluation of Xist RNA transcript levels

We first evaluated the influence of different amounts (20 ng, 200 ng and 2000 ng) of RNA template from a 40,XX mouse (high level of *Xist* RNA transcripts) in a reverse transcription reaction on PCR effectiveness. As shown in **Figure 3d**, both 2000 ng and 200 ng of RNA had a repressive effect. Therefore, 20 ng of RNA template was used for reverse transcription to evaluate the range of the $\Delta Cq_{Xist - Actb}$ values for 40,XX and 40,XY mouse samples (no or low level of *Xist* RNA transcripts). As shown in **Figure 3e**, the range of the $\Delta Cq_{Xist - Actb}$ values for the sixteen 40,XX and 40,XY mouse samples was distinct from each other. The mean $\Delta Cq_{Xist - Actb}$ value (6.05) of the maximum for the 40,XX samples and the minimum for the 40,XY samples was used as the cutoff value for differentiating *Xist* RNA transcript levels in subsequent experiments.

Breeding of KS mouse models by using results from the established PCR assays

Using the established PCR assays, we bred 40,XX^{Y*} and 41,XXY mice from a pair of 40,XY* and 40,XX mice following the protocol in **Figure 1**. To confirm the reliability of our assays, we performed karyotyping of the target mice candidates (mice in the blue and red circles in **Figure 1**), which were identified by PCR assays. Phenotypic examination of the 40,XX^{Y*} and 41,XXY mice candidates, which were identified by PCR assays, was also performed. As shown in **Figure 4**, the karyotype results confirmed that the target mice were correctly identified by the PCR assays and KS mice (40,XX^{Y*} and 41,XXY mice) were successfully generated. Moreover, phenotypic examination revealed that the 40,XX^{Y*} and 41,XXY mice candidates had small, firm testes and Sertoli cell-only presentation, which were in accordance with their karyotype results (**Figure 5**). Therefore, genetic and phenotypic confirmations demonstrated the practical utility of our assays for reliable KS mouse model breeding.

Figure 4: Karyotypes of the target mice for breeding Klinefelter syndrome mouse models. (**a**) A 40,XX^{Y*} mouse from the second generation. The arrow indicates the X^{Y*} chromosome. (**b**) A 40,XY^{*X} mouse from the second generation. The arrow indicates the Y^{*X} chromosome. (**c**) A 41,XYY^{*X} mouse from the third generation. The arrow indicates the Y^{*X} chromosome. (**d**) A 41,XXY mouse from the fourth generation.

DISCUSSION

Cytogenetic analysis methods with metaphase chromosomes (*e.g.*, karyotyping and FISH) are reliable for identifying chromosomal abnormalities, which is essential to the breeding and study of KS mouse models.[22,23,25,26] However, some technical issues remain to be resolved. For cytogenetic analysis, the sources of metaphase chromosomes are limited to those tissues containing a fraction of cells that are actively undergoing cell division. Therefore, only a few starting materials can be used, including the bone marrow, peripheral blood, and tissue biopsies, such as the tail tip.[25] When analyzing cells derived from the bone marrow, cell culture is not required, and the results can be obtained in 1 day or 2 days. However, the mouse is sacrificed during sampling and cannot be used for subsequent breeding.[25] In contrast, peripheral blood or tail tip sampling does not kill the mouse and thus can be performed before breeding. However, cell culture is required for blood or tissue biopsies, which takes 4–10 days before cytogenetic analysis can be performed.[22,23,26] Moreover, FISH requires an additional 2–3 days for slide aging.[22,23] The long turnaround time of the aforementioned processes limits studies that require rapid identification of chromosomal contents. For example, germ cell loss occurs prenatally, progresses rapidly after birth, and is completed at approximately 10 days of life in KS mice.[23,27] Therefore, the time window for investigating the molecular mechanism of this dynamic pathological

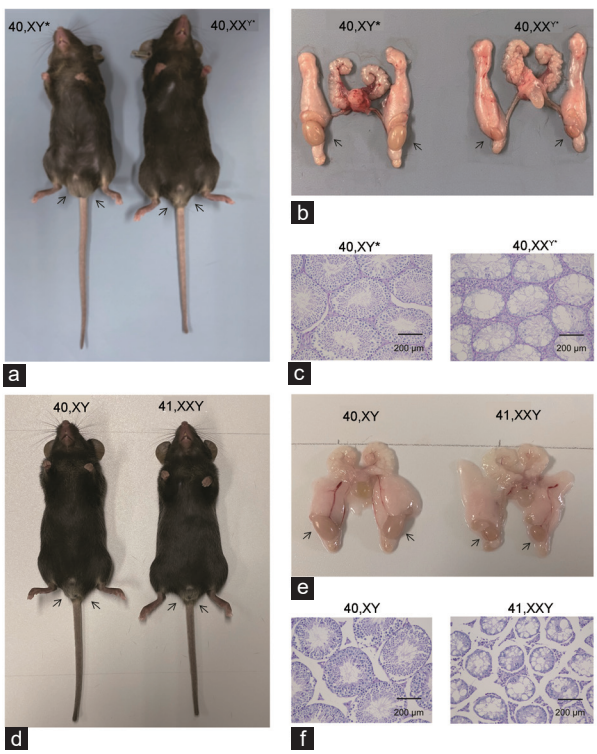

Figure 5: Testicular phenotypes of Klinefelter syndrome mouse models. (**a**) Appearance, (**b**) anatomic analysis, and (**c**) histologic analysis of the testes in a 40,XX^{Y*} mouse and 40,XY* littermate. (**d**) Appearance, (**e**) anatomic analysis, and (**f**) histologic analysis of the testes in a 41,XXY mouse and 40,XY littermate. The arrows indicate the position of the testes. As expected, 40,XX^{Y*} and 41,XXY mice presented small, firm testes. Moreover, the tubule diameters of 40,XX^{Y*} and 41,XXY mice were smaller than those of their reference littermates, germ cells were absent, and only Sertoli cells were observed within the tubules.

change is so narrow that rapid identification (within 1 day) of neonatal KS mice is essential, which poses a technical challenge for cytogenetic methods. In addition to being time-consuming, cytogenetic methods are labor-intensive and technically complicated,[25] thereby reducing their usefulness in large-scale detection, which is generally required to generate enough model mice for study use.

The aforementioned drawbacks of cytogenetic methods can be overcome by molecular methods. PCR is a basic molecular laboratory tool that has demonstrated the ability to detect various types of genetic abnormalities through different data analysis strategies. For example, we can detect the presence or absence of a specific gene region (*e.g.*, azoospermia factor on the Y chromosome) by analyzing amplification profiles,[34] and we can detect numerical changes (*e.g.*, trisomy 21, 47,XXY, or an carrier of spinal muscular atrophy) by analyzing melting profiles or ΔCq values.[9,31,35–37] On the basis of previous studies, we developed three PCR-based assays to detect genetic information related to KS, including the presence or absence of *Sry*, changes in the copy number of *Amelx*, and *Xist* RNA transcript levels in mouse tissue samples. Using these assays, we were able to identify target mice for the breeding of KS models without performing karyotyping or FISH. Compared with karyotyping or FISH, our method is rapid as it takes <1 h for nucleic acid purification, <2 h for reverse transcription, and <2 h for PCR and melting analysis. A short turnaround time for mouse identification is essential for studies focused on rapid physical and pathologic changes in fetal or newborn mice, such as testicular degeneration.[8,23,27] Our method is also inexpensive (<0.5 US dollars per PCR assay), high capacity (up to 96 samples per assay), and easy to perform. Moreover, only 2 ng of DNA and 20 ng of RNA were sufficient to obtain reliable results, suggesting that <0.2 mg of tissue or 1 μl of peripheral blood would be a sufficient sample size and thereby further revealing its utility, especially for the detection of fetal or newborn mice.

An ideal assay for *Sry* identification should only yield a product from male mouse samples with *Sry* but not from female mouse samples without *Sry*; thus, we can identify male mouse samples directly by their amplification profiles. In practice, however, nonspecific amplicons derived from paralogous sequences or primer dimers were difficult to eliminate from reactions with female mouse samples. Because of this, melting profiles are more specific than amplification profiles since the melting profiles of the *Sry* amplicons could be readily differentiated from those of nonspecific amplicons. The amount of DNA template used plays an important role in the melting profiles, and 2 ng was confirmed to be optimal in our study. However, if different PCR reagents are used, the optimal amount of DNA template should be re-evaluated.

Theoretically, after equalizing the DNA template input for the *Amelx* assay, samples with different *Amelx* copy numbers should generate different ranges of Cq values. Therefore, we could infer the *Amelx* copy number in a mouse sample by its Cq value. In practice, we confirmed this assumption (data not shown). However, to further diminish the potential effects of slight differences (*e.g.*, differences in the quantity or quality of DNA template) between samples, *Actb* was used as a reference gene to calibrate the *Amelx* quantification. Accordingly, instead of ranges of Cq values, the ranges of $\Delta Cq_{Amelx\ -\ Actb}$ values were established to quantify *Amelx* in unknown samples. Moreover, rather than using confidence intervals for the different ranges of $\Delta Cq_{Amelx\ -\ Actb}$ values, we used a single cutoff value to determine the *Amelx* copy number, which simplified the data analysis.

The underlying principle of the assay used to determine *Xist* RNA transcript levels was identical to that of *Amelx* quantification. Similarly, a large amount of nucleic acid template had a repressive effect on PCR amplification. We further evaluated whether the repressive effect was derived from the large amount of RNA or the resulting cDNA. The results suggested that the repressive effect was greater for large amounts of RNA (data not shown). Therefore, a smaller amount of RNA was preferable for reverse transcription, which was sufficient to reliably determine *Xist* RNA transcript levels.

In conclusion, we developed three PCR-based assays to facilitate the breeding and study of KS mouse models. Our method is rapid, inexpensive, high capacity, and easy to perform, and only requires small sample amounts. We confirmed the utility of our assays for the successful generation of KS mouse models. We believe that our method will help advance the knowledge of the pathological mechanism of KS.

AUTHORS CONTRIBUTIONS

HXZ and YLZ participated in the study design, establishment of PCR assays, and revising the manuscript. WYX participated in the study design and establishment of PCR assays. XLC, JYJ, XMZ, ZGW, and RQK participated in KS mouse model breeding. QWG conceived of the study, participated in its design and coordination, and drafted the manuscript. All authors read and approved the final manuscript.

COMPETING INTERESTS

All authors declare no competing interests.

ACKNOWLEDGMENTS

We thank the Experimental Teaching Department, School of Medicine, Xiamen University and the Xiamen University Laboratory Animal Center for their kind support of this study.

REFERENCES

1 Klinefelter HF, Reifenstein EC, Albright F. Syndrome characterized by gynecomastia aspermatogenesis without a-leydigism and increased excretion of follicle stimulating hormone. *J Clin Endocrinol Metab* 1942; 2: 615–27.
2 Berglund A, Stochholm K, Gravholt CH. The epidemiology of sex chromosome abnormalities. *Am J Med Genet C Semin Med Genet* 2020; 184: 202–15.
3 Forti G, Corona G, Vignozzi L, Krausz C, Maggi M. Klinefelter's syndrome: a clinical and therapeutical update. *Sex Dev* 2010; 4: 249–58.
4 Gravholt CH, Chang S, Wallentin M, Fedder J, Moore P, *et al*. Klinefelter syndrome: integrating genetics, neuropsychology, and endocrinology. *Endocr Rev* 2018; 39: 389–423.
5 Skakkebaek A, Gravholt CH, Chang S, Moore PJ, Wallentin M. Psychological functioning, brain morphology, and functional neuroimaging in Klinefelter syndrome. *Am J Med Genet C Semin Med Genet* 2020; 184: 506–17.
6 Fjermestad KW, Huster R, Thunberg C, Stokke S, Gravholt CH, *et al*. Neuropsychological functions, sleep, and mental health in adults with Klinefelter syndrome. *Am J Med Genet C Semin Med Genet* 2020; 184: 482–92.
7 Spaziani M, Radicioni AF. Metabolic and cardiovascular risk factors in Klinefelter syndrome. *Am J Med Genet C Semin Med Genet* 2020; 184: 334–43.
8 Willems M, Gies I, Van Saen D. Germ cell loss in Klinefelter syndrome: when and why? *Am J Med Genet C Semin Med Genet* 2020; 184: 356–70.
9 Fu DM, Zhou YL, Zhao J, Hu P, Xu ZF, *et al*. Rapid screening for Klinefelter syndrome with a simple high-resolution melting assay: a multicenter study. *Asian J Androl* 2018; 20: 349–54.
10 Pizzocaro A, Vena W, Condorelli R, Radicioni A, Rastrelli G, *et al*. Testosterone treatment in male patients with Klinefelter syndrome: a systematic review and meta-analysis. *J Endocrinol Invest* 2020; 43: 1675–87.
11 Graham JM Jr, Bashir AS, Stark RE, Silbert A, Walzer S. Oral and written language abilities of XXY boys: implications for anticipatory guidance. *Pediatrics* 1988; 81: 795–806.
12 Gies I, Unuane D, Velkeniers B, De Schepper J. Management of Klinefelter syndrome during transition. *Eur J Endocrinol* 2014; 171: R67–77.
13 Skakkebaek A, Wallentin M, Gravholt CH. Neuropsychology and socioeconomic aspects of Klinefelter syndrome: new developments. *Curr Opin Endocrinol Diabetes Obes* 2015; 22: 209–16.
14 Tournaye H, Krausz C, Oates RD. Concepts in diagnosis and therapy for male reproductive impairment. *Lancet Diabetes Endocrinol* 2017; 5: 554–64.
15 Chang S, Skakkebaek A, Davis SM, Gravholt CH. Morbidity in Klinefelter syndrome and the effect of testosterone treatment. *Am J Med Genet C Semin Med Genet* 2020; 184: 344–55.

16 Gravholt CH, Tartaglia N, Disteche C. Sex chromosome aneuploidies in 2020-the state of care and research in the world. *Am J Med Genet C Semin Med Genet* 2020; 184: 197–201.
17 Winge SB, Soraggi S, Schierup MH, Rajpert-De Meyts E, Almstrup K. Integration and reanalysis of transcriptomics and methylomics data derived from blood and testis tissue of men with 47,XXY Klinefelter syndrome indicates the primary involvement of Sertoli cells in the testicular pathogenesis. *Am J Med Genet C Semin Med Genet* 2020; 184: 239–55.
18 Navarro-Cobos MJ, Balaton BP, Brown CJ. Genes that escape from X-chromosome inactivation: potential contributors to Klinefelter syndrome. *Am J Med Genet C Semin Med Genet* 2020; 184: 226–38.
19 Wistuba J, Beumer C, Brehm R, Gromoll J. 41,XXY* male mice: an animal model for Klinefelter syndrome. *Am J Med Genet C Semin Med Genet* 2020; 184: 267–78.
20 Eicher EM, Hale DW, Hunt PA, Lee BK, Tucker PK, *et al*. The mouse Y* chromosome involves a complex rearrangement, including interstitial positioning of the pseudoautosomal region. *Cytogenet Cell Genet* 1991; 57: 221–30.
21 Cox KH, Bonthuis PJ, Rissman EF. Mouse model systems to study sex chromosome genes and behavior: relevance to humans. *Front Neuroendocrinol* 2014; 35: 405–19.
22 Wistuba J, Luetjens CM, Stukenborg JB, Poplinski A, Werler S, *et al*. Male 41, XXY* mice as a model for Klinefelter syndrome: hyperactivation of leydig cells. *Endocrinology* 2010; 151: 2898–910.
23 Lue Y, Jentsch JD, Wang C, Rao PN, Hikim AP, *et al*. XXY mice exhibit gonadal and behavioral phenotypes similar to Klinefelter syndrome. *Endocrinology* 2005; 146: 4148–54.
24 Aarde SM, Hrncir H, Arnold AP, Jentsch JD. Reversal learning performance in the XY(*) mouse model of Klinefelter and Turner syndromes. *Front Behav Neurosci* 2019; 13: 201.
25 Lee JJ, Warburton D, Robertson EJ. Cytogenetic methods for the mouse: preparation of chromosomes, karyotyping, and *in situ* hybridization. *Anal Biochem* 1990; 189: 1–17.
26 Lue Y, Rao PN, Sinha Hikim AP, Im M, Salameh WA, *et al*. XXY male mice: an experimental model for Klinefelter syndrome. *Endocrinology* 2001; 142: 1461–70.
27 Hunt PA, Worthman C, Levinson H, Stallings J, LeMaire R, *et al*. Germ cell loss in the XXY male mouse: altered X-chromosome dosage affects prenatal development. *Mol Reprod Dev* 1998; 49: 101–11.
28 Vernet N, Mahadevaiah SK, Yamauchi Y, Decarpentrie F, Mitchell MJ, *et al*. Mouse Y-linked *Zfy1* and *Zfy2* are expressed during the male-specific interphase between meiosis I and meiosis II and promote the 2nd meiotic division. *PLoS Genet* 2014; 10: e1004444.
29 Wolstenholme JT, Rissman EF, Bekiranov S. Sexual differentiation in the developing mouse brain: contributions of sex chromosome genes. *Genes Brain Behav* 2013; 12: 166–80.
30 Bustin SA, Benes V, Garson JA, Hellemans J, Huggett J, *et al*. The MIQE guidelines: minimum information for publication of quantitative real-time PCR experiments. *Clin Chem* 2009; 55: 611–22.
31 Guo Q, Zhou Y, Wang X, Li Q. Simultaneous detection of trisomies 13, 18, and 21 with multiplex ligation-dependent probe amplification-based real-time PCR. *Clin Chem* 2010; 56: 1451–9.
32 Keeney S. Meiosis. Volume 2, cytological methods. Preface. *Methods Mol Biol* 2009; 558: v–vi.
33 Committee for the Update of the Guide for the Care and Use of Laboratory Animals. Guide for the Care and Use of Laboratory Animals. 8th ed. Washington: National Academies Press; 2011. p12–15.
34 Guo Q, Lan F, Xu L, Jiang Y, Xiao L, *et al*. Quadruplex real-time polymerase chain reaction assay for molecular diagnosis of Y-chromosomal microdeletions. *Fertil Steril* 2012; 97: 864–9.
35 Guo Q, Xiao L, Zhou Y. Rapid diagnosis of aneuploidy by high-resolution melting analysis of segmental duplications. *Clin Chem* 2012; 58: 1019–25.
36 Xia Z, Zhou Y, Fu D, Wang Z, Ge Y, *et al*. Carrier screening for spinal muscular atrophy with a simple test based on melting analysis. *J Hum Genet* 2019; 64: 387–96.
37 Zhou Y, Xu W, Jiang Y, Xia Z, Zhang H, *et al*. Clinical utility of a high-resolution melting test for screening numerical chromosomal abnormalities in recurrent pregnancy loss. *J Mol Diagn* 2020; 22: 523–31.